European Polymer Journal 195 (2023) 112198

Contents lists available at ScienceDirect

European Polymer Journal

journal homepage: www.elsevier.com/locate/europolj

Exploring inverse vulcanisation mechanisms from the perspective of dark sulfur

Joseph J. Dale [a,*], Joe Stanley [b], Romy A. Dop [a,d], Gabriela Chronowska-Bojczuk [c], Alistair J. Fielding [c], Daniel R. Neill [d,e], Tom Hasell [a,*]

[a] Department of Chemistry, University of Liverpool, Liverpool L69 7ZD, United Kingdom
[b] Department of Chemistry, University of Warwick, Coventry, CV4 7AL, United Kingdom
[c] Centre for Natural Products Discovery, James Parsons Building, Liverpool John Moores University, Byrom Street, Liverpool L3 3AF, United Kingdom
[d] Department of Clinical Infection, Microbiology and Immunology, University of Liverpool, Liverpool L69 7BE, United Kingdom
[e] Division of Molecular Microbiology, School of Life Sciences, University of Dundee, Dundee, DD1 5EH, UK

ARTICLE INFO

Keywords:
Inverse vulcanisation
Sulfur polymer
Bactericidal

ABSTRACT

The build-up of elemental sulfur waste poses problems such that only the advancement of process and product design might act as a solution. Inverse vulcanisation, a process for the generation of high sulfur content polymeric materials may be one such resolution. However, a complete understanding of how these materials form is yet to be fully agreed in this emerging field. Herein is an investigation into the understanding of 'dark sulfur' – amorphous, unreacted sulfur, not incorporated into the polymer backbone – in an attempt to understand further the formation mechanisms behind inverse vulcanisation. This research posits theories regarding polymer formation, thermal rearrangement, and the actions of OH to control the degree of product crosslinking, in relation to the quantity of sulfur unreacted into the polymer structure. The detriments and benefits of this dark sulfur in relation to application and general usage are also investigated, showing that a high content of dark sulfur may encourage planktonic bactericidal activity, while also promoting safety considerations from generated species such as hydrogen sulfide and carbon disulfide, concluded as components of this dark sulfur.

1. Introduction

Naturally occurring elemental sulfur has long played a part in human history, with reference being given as far back as ancient Greece in Homers Odyssey [1]. In modern times sulfur is largely produced as the product of the desulfurization of crude oil [2,3]. Strict rules exist as to the level of sulfur acceptable in gasoline and petroleum-based products, with a maximum of 10 ppm being permitted as of 2017 under the United States Environmental Protection Agencies Tier 3 program [4]. As such this leads to the production of significant quantities of waste sulfur, with up to 7 million tons of excess sulfur produced annually [5]. It has therefore become important to investigate new methods and products that utilize this sulfur, and as such to reduce the build-up of waste. One such process that has gained momentum in recent years is that of inverse vulcanisation (IV). A term coined by Chung *et al.*, inverse vulcanisation involves the ring opening of elemental sulfur followed by reaction with organic co-monomers, resulting in the formation of polymeric materials stabilizing >50 wt% sulfur in a backbone between organic moieties via a process that has the potential to makes use of significant quantities of sulfur waste [6]. The thermal and mechanical characteristics of these materials can be manipulated through alterations in the sulfur loading or crosslinker identity, with lower contents of sulfur and petrochemically sourced co-monomer molecules like dicyclopentadiene (DCPD) [7], ethylidene norbornene (ENB) [8], and divinyl benzene (DVB) [9] presenting a tendency to form materials with a higher glass transition temperature (T_g) and tuneable mechanical properties [10]. Renewable crosslinkers such as myrcene, [11] eugenol, [12] or geraniol [13] often yield lower T_g polymers with an increased flexibility but limited shape persistency. These widely tailorable properties promote a variety of potential applications, with the petrochemically sourced 1,3-diisopropenyl benzene (DIB) demonstrating its use in Li-S batteries [6] and antibacterial applications [14,15], whereas pinene derived monoterpenes such as limonene present application in heavy metal remediation of waste water [16]. Many other polymers have also been applied to these applications in batteries [17–19], antimicrobial [20–22] and water cleaning services [23–26], as well as in IR lenses [27,28] and in

* Corresponding authors.
E-mail addresses: Joseph.Dale@liverpool.ac.uk (J.J. Dale), T.Hasell@liverpool.ac.uk (T. Hasell).

https://doi.org/10.1016/j.eurpolymj.2023.112198
Received 30 March 2023; Received in revised form 25 May 2023; Accepted 30 May 2023
Available online 5 June 2023
0014-3057/© 2023 The Authors. Published by Elsevier Ltd. This is an open access article under the CC BY license (http://creativecommons.org/licenses/by/4.0/).

fire retardant capacities [29,30]. Such is the variability in product formation that minor changes in synthesis conditions can create products of vastly differing properties [31] (see Fig. 1).

While notable research has been directed towards applications and the assessment of new organic co-monomers, fewer investigations have been directed to understand polymer structure or the reaction mechanism [31–34]. Difficulties continue in the analysis of sulfur polymers due to the limited number of analytical techniques available for characterization, the lack of solubility of heavily crosslinked polymers rendering many important techniques such as solution NMR non-applicable. As such the exact polymer structure is challenging to determine, however research into this area continues with Hwang and co-workers suggesting rather than a homogeneous system the presence of both organic and sulfur dominated domains [35]. Previously, differential scanning calorimetry (DSC) [36] or powder x-ray diffraction (PXRD) [37] have been applied to determine if crystalline sulfur is present within the polymer, the common conclusion stating that the absence of crystalline sulfur suggests all available sulfur has been stabilized into the polymer structure. 'Dark sulfur' as recently reported is unpolymerized sulfur existing in an amorphous form that cannot be seen by these pre-established methods [38]. High-performance liquid chromatography (HPLC) was applied to quantify this dark sulfur after extraction from within the polymer structure, adapting a method previously used for the quantification of elemental sulfur in coal [39]. Since this point Raman spectroscopy has also been applied to analyse for the existence of dark sulfur, determining that a sample of S-divinylbenzene prepared with a sulfur loading of 70 wt% contained 11.6% unreacted sulfur [40]. However, it has not been determined as to how this dark sulfur forms, or its identity. Answering these questions may yield important information regarding how these polymeric materials form, and what structure the polymer has at different stages throughout the synthetic process. Discovering routes by which dark sulfur may be controlled, either by promoting formation or hindering it, may prove beneficial to certain applications.

In this work new methods for unpolymerized sulfur quantification are developed, alongside an investigation into the form that dark sulfur takes, how to control dark sulfur formation, and the benefits and detriments of its presence within inverse vulcanised polymers. This in turn reveals information regarding the synthesis mechanism, and the structure of the polymers after reaction and curing. These conclusions then allow the dark sulfur content of sulfur polymers to be intentionally controlled in a way that could benefit certain applications, such as in the inhibition of the growth of planktonic bacterial cells by release of dark sulfurous species into aqueous media. This would be of benefit, as release of planktonic bacterial cells by preestablished bacterial biofilms can lead to dissemination of these bacteria and the generation of new biofilms, thus advancing the growth of bacteria and contributing to the progression of infection or transmission of bacteria to further environments [41–43]. This work demonstrates further the importance of understanding certain process fundamentals when considering inverse vulcanisation.

2. Results and discussion

The analysis of unreacted sulfur in IV polymers has been previously reported, characterized by HPLC methods [38]. However, the details of this "dark sulfur", specifically its' identity, formation, and effects on applications have not yet been discussed. It is prudent to fully understand the answers to these questions if the future commercialization of the IV process is to be successful. Before these questions could be addressed however, it was deemed necessary to develop a new characterization technique for dark sulfur quantification. If used as a metric for polymer product quality control it would be appropriate for analysis to be quick and cheap. UV–Visible (UV–Vis) spectrophotometric methods were therefore developed, allowing for rapid analysis of unreacted sulfur. HPLC systems can be expensive, but benchtop UV–Vis instruments are reasonably priced, and provide rapid absorbance values. The method previously reported using HPLC made use of a diode array detector (DAD) operating at 290 nm ± 20 nm. Elemental sulfur and dark sulfur yield a lambda max within this range (Fig. S1-2).

Using elemental sulfur as a standard allows for the best reference for the photoactive species in dark sulfur, as HPLC analysis demonstrates similar residence times for elemental sulfur and dark sulfur (6.85 and 6.99 min respectively) analysed under the same wavelength (290 nm), also observed in the previous work on this topic [38]. The slight distinction in residence times however does suggest a different composition between elemental and dark sulfur, although due to the variety of species considered under the definition of dark sulfur this comparison would prove the best way to consider all dark sulfurous species in total. This was then compared to a prepared Beer-Lambert plot of absorbance vs concentration of elemental sulfur dissolved in ethyl acetate at concentrations of 0.05 mg mL^{-1} to 0.30 mg mL^{-1}, at 0.05 mg mL^{-1} intervals (Fig. 2). Ethyl acetate was selected as the solvent of choice as it has a lower solubility for sulfur species, so was expected to only extract dark sulfurous species and not oligomeric fractions from within the polymer, and it shows no absorption under UV at the wavelengths of interest unlike the previously reported toluene (figure S3-4). At the solution concentrations required for analysis (1 mg mL^{-1}) elemental sulfur fully dissolves in EtOAc, thus when the dark sulfur solutions are prepared at this concentration of polymer (1 mg polymer undissolved in 1 mL EtOAc) the dark sulfur species would be fully dissolved, as the elemental sulfur at a much higher concentration was dissolved. No dissolution of any of the polymers considered herein was observed in EtOAc. An

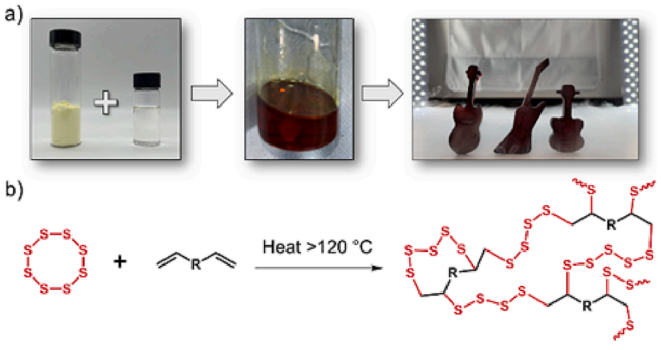

Fig. 1. (a) The components and stages of an inverse vulcanisation reaction, progressing from separate sulfur and crosslinker, to a homogenous prepolymer stage, followed by curing and moulding into various forms. In this case, a 1:1 wt ratio of sulfur to DIB comonomer was used. (b) General reaction scheme of inverse vulcanisation.

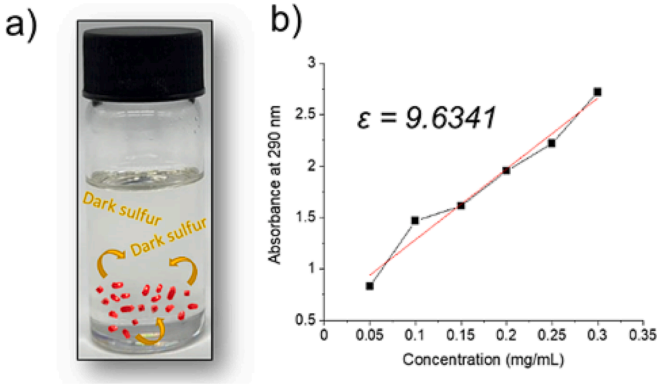

Fig. 2. (a) Pictorial representation of the solvent extraction process of dark sulfur from within the polymer structure into ethyl acetate solvent. (b) Beer-Lambert plot showing the linear increase in absorbance at 290 nm of elemental sulfur solutions with increasing concentration.

extinction coefficient of 9.6341 was determined, allowing for application of the Beer-Lambert law to calculate concentration of dark sulfur (in mg mL^{-1}) after acquisition of the absorbance value. Further calculations yielded the amount of unreacted sulfur in the polymer in wt.% in accordance with Eq. (S1). This method was then applied to all future investigations.

The first question that required answering was that of the identity of dark sulfur. While previously hypothesized to be comprised of unreacted S8 in an amorphous form, polysulfides, and radicals, this was never conclusively established. Analysis of dark sulfur solutions in ethyl acetate firstly by HPLC/MS using an electrospray ionization mass spectrometer were completed. A number of mass peaks were observed (Fig. S5-9), correlating to potential polysulfides or stable radical species. A peak at an m/z value of 55 is cautiously proposed to be a single S atom associated with a positively charged sodium derived from within the mass spectrometer, while a peak at 73 Daltons was ascribed to be hydrogen thioperoxide (HOSH) associated with sodium. The appearance of a peak at 101 Daltons (mass spectra analysed in negative mode, actual $m/z = 102$) was tentatively ascribed to be a cluster of 3 H2S molecules.

Further mass spectrometry analysis was conducted using a Waters Xevo G2-XS QToF with Acquity UPC (ToF) (Fig. S10). Dark sulfur samples of the vitrified polymers prepared at 165 °C were analysed. Species identified include thiols and sulfur rings, specifically S6 and S8 in an amorphous form. This is an important determination when considering both how the IV reaction progresses, and the potential applications for these materials in the future. CS2, a dangerous neurotoxin [44], was also observed in this analysis. While likely only present in small quantities, its presence must be noted for product safety purposes, an argument that could similarly be made for thiols as they may progress further to form hydrogen sulphide, a toxic gas that can be fatal even in low concentrations [45]. Dark sulfur therefore confers an issue regarding safety in addition to that of altering polymer properties. If there is a large quantity of unpolymerized sulfur in a polymer then the thermal and mechanical properties may be altered due to the change in the potential length of the polymer backbone. It is therefore key to investigate the formation mechanisms of dark sulfur in IV polymers. A series of parameters were subsequently altered for IV reactions including reaction time, reaction temperature, curing time, catalyst presence and reaction speed, and product washing.

Electron paramagnetic resonance (EPR) spectroscopy was also conducted on both polymer and dark sulfur samples (Fig. S11-12) to determine if unreacted sulfurous based radical species that could react further to generate more of these dangerous species were present. Polymer samples were prepared at varying reaction temperatures of 135, 165, and 195 °C, with dark sulfur samples prepared from these polymers. No radical species were observed at room temperature by EPR analysis in dark sulfur solutions prepared in hexane (hexane selected as it is a non-polar solvent for use in EPR that also has solubility for sulfurous species without solubilizing the polymer), suggesting that dark sulfur does not contain any thiyl radicals. The 3 S-DIB (50 wt% sulfur, 50 wt% DIB) polymer samples each gave an EPR signal similar to that observed by Wadi *et al.*, consisting of a structure-less derivative with g 2.0046 [46]. Dong and co-workers suggest this g value corresponds to polyenyl radicals, generated by allylic proton abstraction [47]. A comparison was conducted between washed (hexane wash solution) and unwashed polymers (Fig. S13). No change in radical signal was observed in the EPR trace, thus suggesting that this radical signal is conferred by the organic section of the polymer, in agreement with the research completed by Wadi *et al.* This radical species remained stable and persistent after 50 days of aging (Fig. S14-15).

In a consideration to firstly understand the formation of dark sulfur, alterations in reaction time and temperature were considered. Three reaction temperatures were considered (135, 165, and 195 °C), with samples being taken throughout the prepolymer state until vitrification. No crystalline sulfur was observed by DSC analysis in any sample considered (Fig. S16-31). It was observed that reaction time has no clear correlation to the formation of dark sulfur, therefore suggesting that the formation of dark sulfur in the reaction progress is random, with large degrees of rearrangement between polymeric and dark sulfurous states. The high reaction temperature encourages a larger degree of polysulfide chain breakdown, forming a higher quantity of shorter chain polysulfides that may react with organic sections to form highly crosslinked sections. This in turn leads to a higher incidence of collision between sulfur radicals and olefinic crosslinking points, resulting in a much faster reaction. This faster reaction of shorter polysulfides yields a much higher T_g product due to the shorter polymer chains and thus reduced chain mobility, while a lower temperature promotes a slower reaction and less sulfur chain breakdown, allowing longer chains to be incorporated into the polymer backbone. This reduces the quantity of unreacted sulfur, and increases chain mobility thus decreasing the T_g (Fig. S32). This would therefore suggest that while reaction time presents no correlation to unreacted sulfur, reaction speed has a notable effect. This dark sulfur can be washed out of the polymer into solvents with good solubility for sulfur with no detriment to the polymer properties (Fig. S33-35). Hexane is selected as it does not damage the polymer structure but maintains reasonable sulfur solubility. Washing of the vitrified samples at each reaction temperature before TGA showed no decrease in the mass loss of sulfur (determined by TGA wherein the sample is heated to 600 °C at 10 °C min^{-1}, with sulfur decomposition mass loss occurring at approximately 220 °C, see SI for details) in the sample prepared at 135 °C upon decomposition of sulfur, an expected result as there is no free unpolymerized sulfur to be removed via washing. The percentage change in mass loss decreases for the samples prepared at 165 °C (2.0% less mass lost on decomposition), and 195 °C (3.2% less mass lost on decomposition) (Figs. 3, S36-37). This data echoes the increasing amount of dark sulfur found to be present at elevated reaction temperatures. Not all dark sulfur has been removed, predicted to be due to the solubility of sulfur in hexane as only a single wash was conducted, and the diffusion rate of sulfur out of the polymer structure into the solvent. Polymer curing time allows for different properties due to structure rearrangement [48]. Upon reaching a prepolymer state the solution can be poured into a silicone mould and cured in an extracted oven at elevated temperature. S-DIB prepolymers were sampled at the start of the prepolymer window. These samples were then left to cure for different lengths of time between 1 and 96 h. Fig. 4 shows firstly a direct inverse correlation between dark sulfur and T_g, signalling to the effects of sulfur chain length and structure on the polymer properties. In the first 5 h a rapid increase in T_g and decrease in dark sulfur are observed. This is predicted to be due to rearrangement of the polymer chains into a more crosslinked state, while incorporating all the sulfur into the polymer backbone, made possible by the dynamic S-S linkages breaking and reforming. This yields a highly crosslinked product. From this point onwards the T_g decreases and dark sulfur increases. This is predicted to be due to rearrangement into a more thermodynamically favoured branched state, with sulfur loops and branching points becoming more prominent over crosslinking, thus increasing dark sulfur as it is released from the crosslinked structure. Onose *et al.* posit that continued heating can results in an increase in the terminal character of the polymers, with 1,2-dithiol-3-thione ring systems and terminal methyl groups suggested as terminating groups [49]. This suggestion of methyl terminating groups is echoed by Pyun *et al.*, along with thiol groups also [50]. It is hypothesized that rearrangement of the polymer structure in the first 24 h causes the creation of 'trailing arms' and unbound polysulfides that contribute to the dark sulfur content analysed. These "trailing arms", while part of the polymer structure, may break off upon addition of solvent due to the weaker S-S bonds present compared to a chain stabilized between stronger C-S bonds, and subsequently inflate the dark sulfur quantity. The solubility in THF after 24 h remained low for the 5 h cured sample before gradually increasing until after 48 h of curing the samples were fully soluble, confirming that the prolonged application of heat causes rearrangement into a more linear and therefore soluble form, likely contributed to by the formation

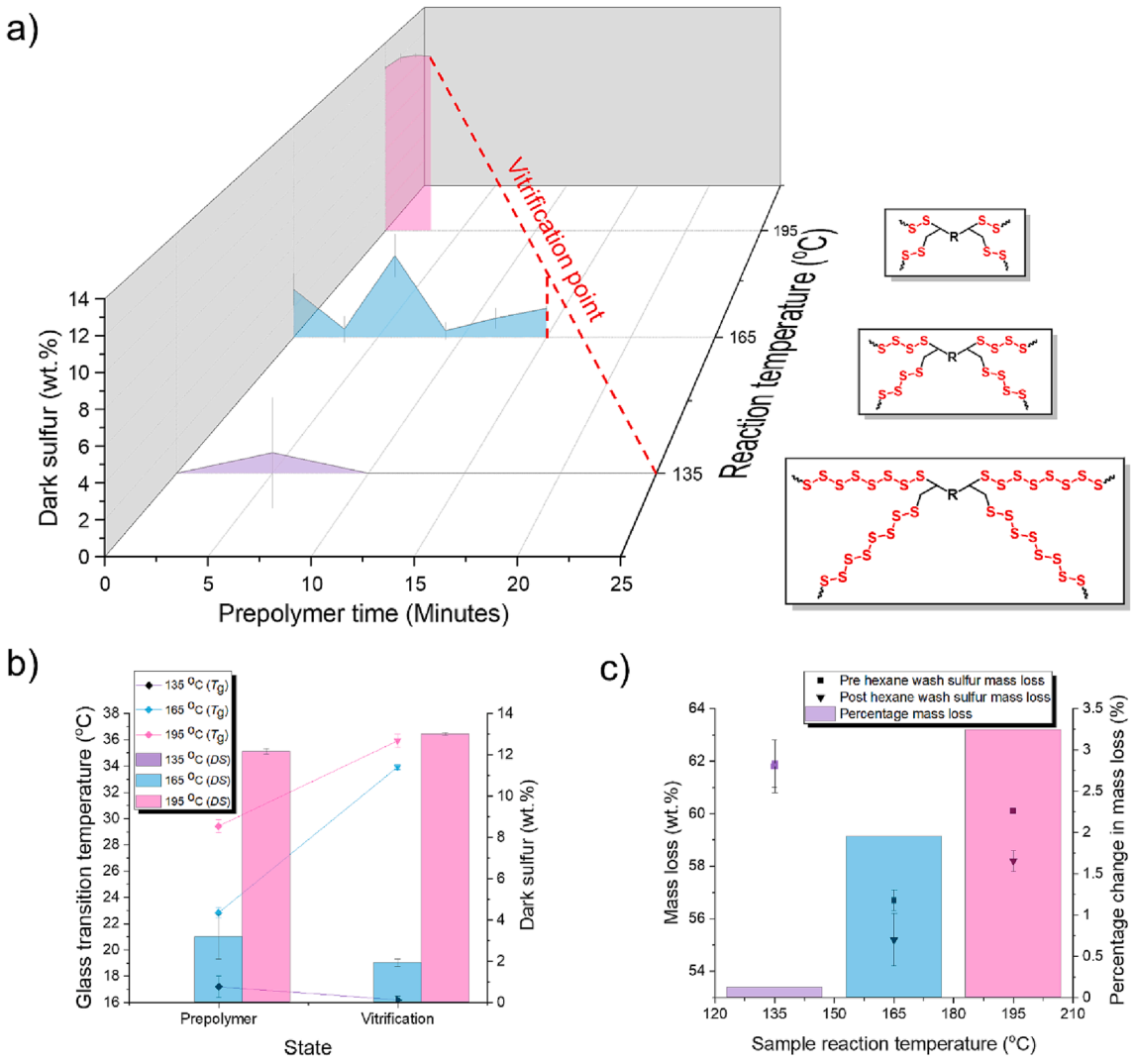

Fig. 3. (a) The change in dark sulfur quantity throughout the prepolymer window until vitrification of reactions carried out with a 1:1 wt ratio of sulfur to DIB comonomer for 3 different reaction temperatures. The data suggest that higher reaction temperatures lead to increased generation of dark sulfur, hypothesized to be due to creation of many short chain polysulfides as represented in the structures suggested. This increases the incidence of collision and thus the rate of reaction. (b) The difference in dark sulfur and T_g between prepolymer and vitrified polymer states. (c) The change in mass loss of the sulfur decomposition transition acquired by TGA and percentage mass loss comparing washed and unwashed polymers for each of the considered reaction temperatures.

of trailing arms and sulfur loops. This was then repeated for two other polymers, the renewably sourced limonene and petrochemical ENB. Both however showed a different relationship, wherein dark sulfur shows a relative increase within the first 5 h, before a decrease to a relative plateau. Both interestingly provide lower dark sulfur levels than DIB after 48 h of curing. The previous report considering dark sulfur showed limonene presenting higher levels of dark sulfur compared to DIB, however this was only considered after 24 h curing whereas on this occasion it would appear that limonene may indeed stabilize more sulfur within the polymer structure after 24 h curing than DIB. Therefore, the ability to tailor these polymers with regards to dark sulfur is easily conducted through alterations in curing time, but first requires an understanding of the polymer behaviour.

Catalysts have previously been reported to accelerate the rate of reaction in IV polymers [32,51]. In order to understand how reaction speed affects dark sulfur formation a number of catalysts representing a wide range of reaction times were selected from the work completed by Dodd et al. [51]. Operating under the assumption that the IV reaction occurs, at least in part, through a radical mechanism, (2,2,6,6-tetramethylpiperidin-1-yl)oxyl (TEMPO) was also used in this study with the expectation of its' action as a radical scavenger, thus slowing down the rate of reaction, potentially promoting the generation of dark sulfur as the sulfur may not be stabilized into the polymer structure with decreased radical action. Contrary to this hypothesis, TEMPO acted as a catalyst, rapidly accelerating the reaction rate, catalysing the reaction to a similar degree as Na(DEDC). It is theorized that TEMPO stimulates a radical type mechanism and acts here as an initiator to accelerate the reaction and the breakdown of polysulfide chains as would be conferred by a higher reaction temperature. The application of catalysts resulted, in all cases, in an increase in generated dark sulfur (Fig. 5a). This could be due to the break-down of the sulfur chains causing the same effect observed by increasing the reaction temperature. A higher temperature or the use of a catalyst leads to the breakdown of sulfur chains into shorter polysulfides, increasing the incidence of collision and increasing the rate of reaction.

However, while no increase in reaction rate was observed for NaOH, a dramatic increase in dark sulfur formation was observed. A comparison of the FTIR spectra of reactions with and without NaOH added showed a weak peak arising at 1683 cm^{-1}, ascribed to a conjugated carbonyl group, and strengthened peaks appearing at 1124 cm^{-1} and 1003 cm^{-1} corresponding to C-O stretching (Figs. 5b, S38). It is hypothesized therefore that OH radicals may also partake in the IV

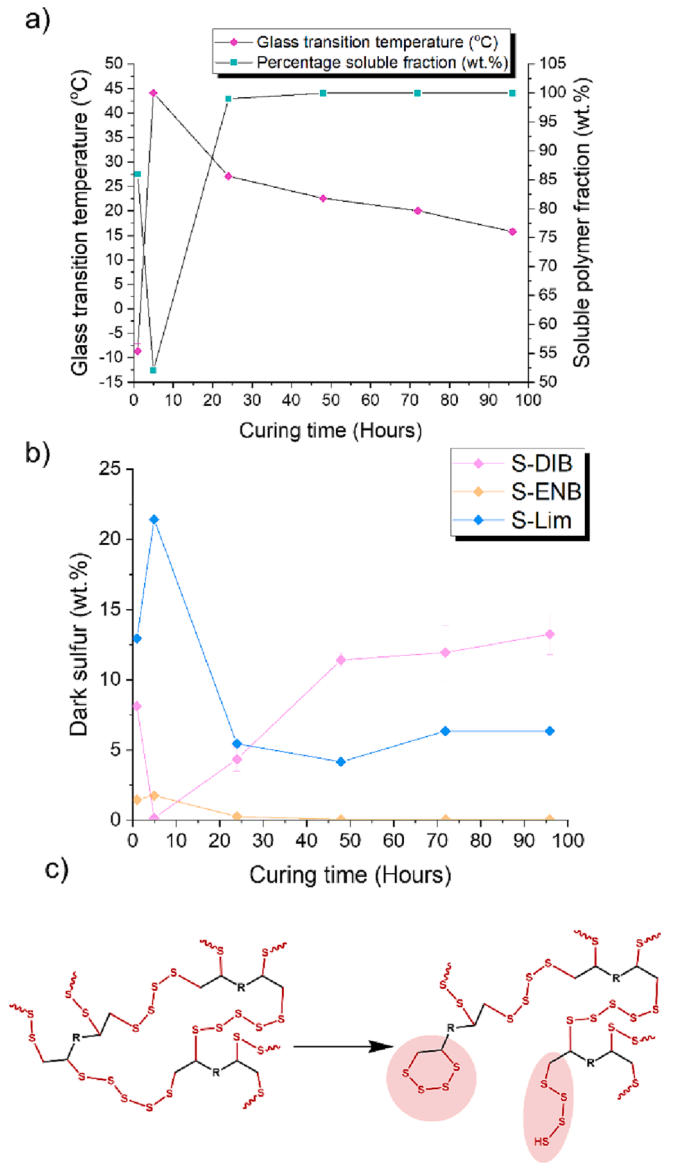

Fig. 4. (a) Change in T_g and solubility in THF of S-DIB polymers with curing time. (b) The change in dark sulfur over curing times of up to 96 h for S-DIB, S-ENB, and S-Limonene. While dark sulfur increases in the first 5 h before decreasing and plateauing for the latter 2 polymers, S-DIB shows the opposite, proposed as due to the rearrangement to a more linear structure. (c) Suggested structure of "trailing arms" theory that promotes linearity while increasing dark sulfur generation. Highlighted in red show the concepts of (left) sulfur looping and (right) trailing arms. (For interpretation of the references to colour in this figure legend, the reader is referred to the web version of this article.)

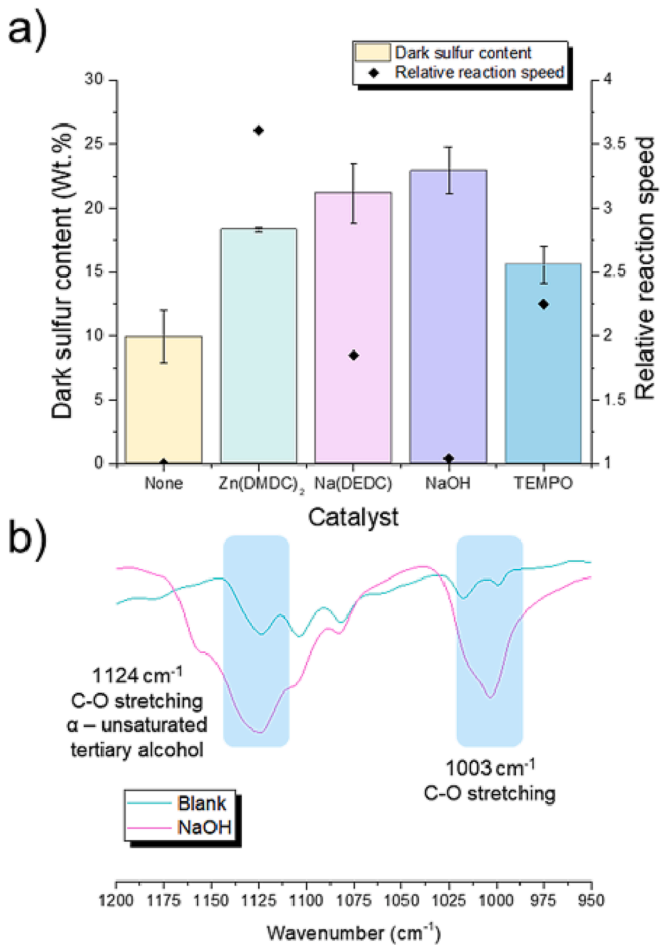

Fig. 5. (a) Comparison of the quantity of dark sulfur generated by the addition of catalysts at 10 wt% loading, showing that all catalysed reactions generate more unreacted amorphous polysulfides. The relative reaction rate of each catalysed reaction to the uncatalyzed analogue reaction is also given, calculated by the timing of each reaction from addition of comonomer to vitrification. (b) FTIR spectra of a reaction under standard conditions (blank) and a reaction with 15 wt% NaOH loading showing an increase in intensity of the peaks at 1124 $cm^{-1}$and 1003 cm^{-1}, correlating to C-O bind formation.

reaction, generated from present moisture or the addition of NaOH. This results in terminal C=O or OH groups that occupy potential crosslinking points. This would increase dark sulfur and polymer linearity, as a reduced quantity of sulfur can be stabilized into the polymer structure. A series of reactions were conducted increasing the loading of NaOH (0, 1, 5, 10, 15 wt%), (Fig. 6a). The solubility and dark sulfur increased with increasing NaOH loading, suggesting the formation of more linear sections as hydroxide species move to occupy crosslinking sites before sulfur chains. The colour of these polymers progresses from a black opaque solid to a more translucent red with increasing NaOH loading (Fig. 6b). It is tentatively suggested that the colour of these polymers derives in part from the interaction of light with the C-S bond, thus a colour change is observed as C-S bond formation is replaced with C-O bond formation. This conclusion regarding the loading of NaOH could be useful for tailoring polymer properties, particularly with respect to any application relating to optics e.g. high-refractive index lenses, [52,53] as it may allow for a specific degree of lens transparency by loading of an optimized quantity of NaOH.

In this consideration, the appearance of these FTIR peaks when no NaOH is present would suggest that there is potential for moisture in the air, or trapped moisture in the sulfur powder, to contribute to the IV reaction mechanism. Comparison of FTIR spectra of the samples prepared at varying reaction temperatures also shows an increase in OH and C-O stretching at lower reaction temperatures, suggesting that with a longer reaction time there is more opportunity for moisture to partake in the reaction and block crosslinking sites (Fig. S39-41). Selected ion flow tube mass spectrometry (SIFT-MS) headspace analysis under nitrogen of IV reactions with and without drying of sulfur powder under vacuum for 24 h showed that without drying a greater quantity of hydrogen sulphide gas is evolved (Fig. S42). H2S gas is commonly thought to generate from the hydrogen abstraction of olefinic protons by sulfur acting to initiate the IV reaction [31]. The SIFT-MS analysis thus suggests that hydrogen abstraction also occurs from environmental moisture. Water may therefore act as an initiating species for the IV reaction, with a notable observation being that under open conditions the reaction progresses at a much faster rate than under a controlled nitrogen

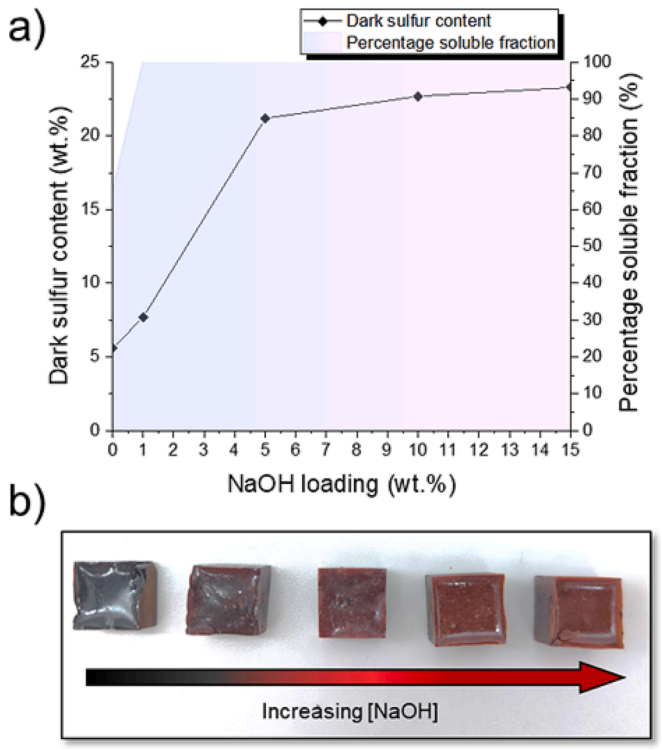

Fig. 6. (a) The changes in dark sulfur content and percentage soluble fraction of S-DIB polymers with increasing concentrations of added NaOH. (b) Picture of polymers with increasing concentration of NaOH between 0, 1, 5, 10, and 15 wt %. All polymers were moulded into 1 cm^3 shapes.

atmosphere, yielding average prepolymer window times to reach vitrification of 13.0 and 17.4 min respectively. This conclusion would state that the humidity and moisture content of the IV reaction should be controlled, in order to increase repeatability and prevent the terminal OH blocking of crosslinking sites.

Understanding the consequences of dark sulfur formation is key, as previously mentioned mass spectrometry suggests the presence of dangerous sulfur containing species. However, the benefits of these unreacted sulfurous species should not be overlooked, such is to say that dark sulfur could act as a sulfurous reservoir, useful in an antibacterial capacity. A series of S-DIB polymers were therefore synthesized as 1 cm^3 and split into 3 sets, with no crystalline sulfur present in any samples (Fig. S43). The antibacterial activity of the materials was evaluated against a methicillin-resistant *Staphylococcus aureus* (USA300), a Gram-positive bacterium that causes significant numbers of global infections annually [54]. The first set were tested as made. The second set were washed in deionized (DI) water for 7 days, while the third set were washed in hexane for 6 days, before washing with water for 1 day to remove any residual hexane that may contribute to the bactericidal effects. These polymers were then left to dry and evacuate residual water, before testing against *S. aureus* (Fig. 7).

The inhibitory effect of the samples against planktonic *S. aureus* was found to decrease compared to the unwashed sample. The washing process removes dark sulfur species that, upon entering the water-based growth medium, may have an inhibitory effect against viable *S. aureus* cells. No difference in the change in the number of surface associated cells before and after washing was observed, suggesting a different mechanism by which bacteria are killed in this instance. The observed surface inhibitory effect could be due to the sulfur chains within the polymer structure. Naturally therefore the surface effect would remain unchanged following a period of washing, as the polymer structure is unaffected during this procedure. A greater decrease in efficacy is observed in the set of samples washed in hexane, showing that hexane is

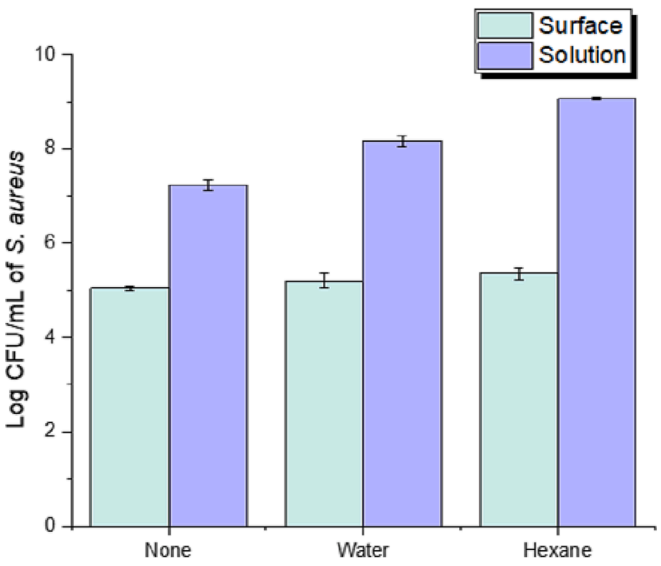

Fig. 7. The demonstrable impact of removing dark sulfur by washing with water and hexane on the antibacterial capacity of IV polymers, with reduced inhibitory effect for planktonic (solution) cells after 5 h incubation. *$p < 0.05$, **$p < 0.001$ relative to unwashed sample.

a much more proficient washing solvent compared to water. However, these data also show the potential for the use of water as a less efficient washing medium for dark sulfur.

3. Conclusions

An investigation into the formation, identity, and benefits and detriments of unreacted amorphous "dark" sulfur has been conducted, with UV–Vis spectrophotometry applied to assist in dark sulfur quantification. The presence of a series of sulfurous ring species (e.g. S_6, S_8), carbon disulphide, hydrogen sulphide, and thiols in dark sulfur present key safety concerns for any large-scale production of inverse vulcanised polymers, though methods of removal such as polymer washing, or production control e.g. lower reaction temperatures, controlled curing, etc. allow for this issue to be negated. The benefits of dark sulfur in the inhibition of planktonic bacterial cells are also demonstrated, with the potential to increase dark sulfur production by e.g. higher reaction temperatures, use of catalysts, or the application of NaOH in order to potentially further this antibacterial effect. Research also indicates the interaction of water, specifically OH species, in the inverse vulcanisation mechanism, with potential crosslinking manipulation and colour tuning conferred through the use of NaOH, while the drying of sulfur can decrease the production of hydrogen sulphide during the synthesis. Therefore, it is believed that the research conducted herein provides further steps towards control of the inverse vulcanisation process, and a new paradigm for the tailoring of bespoke high-sulfur content polymeric materials. The advancement of the understanding of IV promotes greater benefit to this green solution to the waste sulfur problem.

Author Contributions

The work was conceived by JD. Work was conducted by JD and JS, antibacterial analysis was conducted by RD and DN, EPR analysis was conducted by GCB and AF. TH acted as research director. All authors have given approval to the final version of the manuscript.

CRediT authorship contribution statement

Joseph J. Dale: Conceptualization, Methodology, Validation, Formal analysis, Investigation, Writing – original draft, Writing – review & editing, Visualization. **Joe Stanley:** . **Romy A. Dop:** Investigation, Visualization, Writing – review & editing. **Gabriela Chronowska-**

Bojczuk: Investigation, Visualization, Writing – review & editing. **Alistair J. Fielding:** Project administration, Funding acquisition, Supervision, Writing – review & editing, Conceptualization. **Daniel R. Neill:** Project administration, Funding acquisition, Supervision, Writing – review & editing, Conceptualization. **Tom Hasell:** Project administration, Funding acquisition, Supervision, Writing – review & editing, Conceptualization.

Declaration of Competing Interest

The authors declare that they have no known competing financial interests or personal relationships that could have appeared to influence the work reported in this paper.

Data availability

Data will be made available on request.

Acknowledgements

We thank Alexander Ciupa for HPLC-MS and UV-Vis support, Krzysztof Pawlak for UV-Vis support, and Steven Robinson for MALDI-TOF support. We thank Veronica Hanna and William Sandy for assistance in figure design. We thank Douglas Parker and Element for access to SIFT-MS, and Sam Petcher for useful conversations. JD thanks ARKEMA for sponsoring his PhD. JS thanks the Leverhulme foundation for funding his summer project. TH is a Royal Society University Research Fellow. DN holds a Sir Henry Dale Fellowship awarded by the Welcome Trust and the Royal Society (Grant Number 204457/Z/16/Z).

Tom Hasell reports financial support was provided by The Royal Society. Joe Stanley reports financial support was provided by Leverhulme Trust. Daniel Neill reports financial support was provided by The Royal Society. Joseph Dale reports financial support was provided by Arkema

Appendix A. Supplementary material

Supplementary data to this article can be found online at https://doi.org/10.1016/j.eurpolymj.2023.112198.

References

[1] Homer, The Odyssey, W. Heinemann, G.P. Putnam's sons, London, New York, 1919.
[2] M. Yaseen, S. Khattak, S. Ullah, F. Subham, W. Ahmad, M. Shakir, Z. Tong, Chem. Eng. Res. Des. 179 (2022) 107–118.
[3] A.C. Byrns, W.E. Bradley, M.W. Lee, Ind. Eng. Chem. 35 (1943) 1160–1167.
[4] E.P. Agency, Fed. Reg. (2014) 79.
[5] G. Kutney, Sulfur, History, Technology, Applications and Industry, ChemTec Publishing, 2007.
[6] W.J. Chung, J.J. Griebel, E.T. Kim, H. Yoon, A.G. Simmonds, H.J. Ji, P.T. Dirlam, R. S. Glass, J.J. Wie, N.A. Nguyen, B.W. Guralnick, J. Park, A. Somogyi, P. Theato, M. E. Mackay, Y.E. Sung, K. Char, J. Pyun, Nat. Chem. 5 (2013) 518–524.
[7] D.J. Parker, H.A. Jones, S. Petcher, L. Cervini, J.M. Griffin, R. Akhtar, T. Hasell, J. Mater. Chem. A 5 (2017) 11682–11692.
[8] J.A. Smith, X.F. Wu, N.G. Berry, T. Hasell, J. Polym. Sci. Part a-Polym. Chem. 56 (2018) 1777–1781.
[9] I. Gomez, D. Mecerreyes, J.A. Blazquez, O. Leonet, H.B. Youcef, C. Li, J.L. Gómez-Cámer, O. Bondarchuk, L. Rodriguez-Martinez, J. Power Sources 329 (2016) 72–78.
[10] V. Hanna, P. Yan, S. Petcher, T. Hasell, Polym. Chem. 13 (2022) 3930–3937.
[11] I. Gomez, O. Leonet, J.A. Blazquez, D. Mecerreyes, ChemSusChem 9 (2016) 3419–3425.
[12] A. Hoefling, D.T. Nguyen, Y.J. Lee, S. Song, P. Theato, Mater. Chem. Front. 1 (2017) 1818–1822.
[13] C.P. Maladeniya, M.S. Karunarathna, M.K. Lauer, C.V. Lopez, T. Thiounn, R. C. Smith, Mater. Adv. 1 (2020) 1665–1674.
[14] J.A. Smith, R. Mulhall, S. Goodman, G. Fleming, H. Allison, R. Raval, T. Hasell, ACS Omega 5 (2020) 5229–5234.
[15] R.A. Dop, D.R. Neill, T. Hasell, Biomacromolecules 22 (2021) 5223–5233.
[16] M.P. Crockett, A.M. Evans, M.J.H. Worthington, I.S. Albuquerque, A.D. Slattery, C. T. Gibson, J.A. Campbell, D.A. Lewis, G.J.L. Bernardes, J.M. Chalker, Angew. Chem.-Int. Ed. 55 (2016) 1714–1718.
[17] P.T. Dirlam, A.G. Simmonds, T.S. Kleine, N.A. Nguyen, L.E. Anderson, A.O. Klever, A. Florian, P.J. Constanzo, P. Theato, M.E. Mackay, R.S. Glass, K. Char, J. Pyun, RSC Adv. 5 (2015) 24718–24722.
[18] S. Shukla, A. Ghosh, U.K. Sen, P.K. Roy, S. Mitra, N. Lochab, ChemistrySelect 1 (2016) 594–600.
[19] B. Oschmann, J. Park, C. Kim, K. Char, Y.-E. Sung, R. Zentel, Chem. Mater. 27 (2015) 7011–7017.
[20] Z.L. Deng, A. Hoefling, P. Theato, K. Lienkamp, Macromol. Chem. Phys. 219 (1700497) (2018) 1–6.
[21] J. Cubero-Cardoso, P. Gómez-Villegas, M. Santos-Martín, A. Sayago, Á. Fernández-Recamales, R. F. d. Villarán, A. A. Cuadri, J. E. Martín-Alfonso, R. Borja, F. G. Fermoso, R. León, J. Urbano, Polym. Test. 109 (2022) 1–8.
[22] V.S. Wadi, K.K. Jena, K. Halique, S.M. Alhassan, ACS Appl. Polym. Mater. 2 (2020) 198–208.
[23] S. Petcher, B. Zhang, T. Hasell, Chem. Commun. 57 (2021) 5059–5062.
[24] N.A. Lundquist, J.M. Chalker, Sustain. Mater. Technol. 26 (2020) e00222.
[25] N.A. Lundquist, M.J.H. Worthington, N. Adamson, C.T. Gibson, M.R. Johnston, A. V. Ellis, J.M. Chalker, RSC Adv. 8 (2018) 1232–1236.
[26] J.M. Scheiger, C. Direksilp, P. Falkenstein, A. Welle, M. Koenig, S. Heissler, J. Matysik, P.A. Levkin, P. Theato, Angew. Chem. 59 (2020) 18639–18645.
[27] J. Kuwabara, K. Oi, M.M. Watanabe, T. Fukuda, T. Kanbara, ACS Appl. Polym. Mater. 2 (2020) 5173–5178.
[28] D. Boyd, V.Q. Nguyen, C. McClain, F.H. Kung, C.C. Baker, J.D. Myers, M.P. Hunt, W. Kim, J.S. Sanghera, ACS Macro Lett. 8 (2019) 113–116.
[29] I.B. Najmah, N.A. Lundquist, M.K. Stanfield, F. Stojcevski, J.A. Campbell, L. J. Esdaile, C.T. Gibson, D.A. Lewis, L.C. Henderson, T. Hasell, J.M. Chalker, ChemSusChem 14 (2021) 2352–2359.
[30] K.-S. Kang, A. Phan, C. Olikagu, T. Lee, D. A. Loy, M. Kwon, H.-j. Paik, S. J. Hong, J. Bang, W. O. P. Jr., M. Sciarra, A. R. d. Angelis and J. Pyun, Angew. Chem.-Int. Ed. 60 (2021) 22900–22907.
[31] K. Orme, A.H. Fistrovich, C.L. Jenkins, Macromolecules 53 (2020) 9353–9361.
[32] X. Wu, J.A. Smith, S. Petcher, B. Zhang, D.J. Parker, J.M. Griffin, T. Hasell, Nat. Commun. 10 (2019) 647.
[33] M.J.H. Worthington, R.L. Kucera, J.M. Chalker, Green Chem. 19 (2017) 2748–2761.
[34] Y.Y. Zhang, J.J. Griebel, P.T. Dirlam, N.A. Nguyen, R.S. Glass, M.E. Mackay, K. Char, J. Pyun, J. Polym. Sci. Part a-Polym. Chem. 55 (2017) 107–116.
[35] J.H. Hwang, S.H. Kim, W. Cho, W. Lee, S. Park, Y.S. Kim, J.-C. Lee, K.J. Lee, J. J. Wie, D.-G. Kim, Adv. Opt. Mater. 2202432 (2023) 1–9.
[36] S.F. Valle, A.S. Giroto, R. Klaic, G.G.F. Guimaraes, C. Ribeiro, Polym. Degrad. Stab. 162 (2019) 102–105.
[37] M. Arslan, B. Kiskan, Y. Yagci, Macromolecules 49 (2016) 767–773.
[38] J.J. Dale, S. Petcher, T. Hasell, ACS Appl. Polym. Mater. 4 (2022) 3169–3173.
[39] D.H. Buchanan, K.J. Coombs, P.M. Murphy, Energy Fuel (1993) 219–221.
[40] L.J. Dodd, C. Lima, D. Costa-Milan, A.R. Neale, B. Saunders, B. Zhang, A. Sarua, R. Goodacre, L.J. Hardwick, M. Kuball, T. Hasell, Polym. Chem. 14 (2023) 1369–1386.
[41] L.A. Pratt, R. Kolter, Mol. Microbiol. 30 (1998) 285–293.
[42] M. Kostakioti, M. Hadjifrangiskou, S.J. Hultgren, Cold Spring Harb. Perspect. Med. 3 (2013) 1–23.
[43] R.D. Monds, G.A. O'Toole, Trends in Mircrobiology (2009) 73–87.
[44] M. Davidson, M. Feinleib, Am. Heart J. 83 (1972) 100–114.
[45] B. Ramazzini, *Diseases of Workers (Transl. from the Latin text De Morbis Artificum by W. C. Wright. 1940)*, Univ. Chicago Press, Chicago, Reprinted in History Med, Vol. 23 edn., 1713.
[46] V.K.S. Wadi, K.K. Jena, S.Z. Khawaja, K. Yannakopoulou, M. Fardis, G. Mitrikas, M. Karagianni, G. Papavassiliou, S.M. Alhassan, Acs Omega 3 (2018) 3330–3339.
[47] D. Wang, Z. Tang, Y. Liu, B. Guo, Green Chem. 22 (2020) 7337–7342.
[48] N. Han, W. Cho, J.H. Hwang, S. Won, D.-G. Kim, J.J. Wie, Polym. Chem. 14 (2023) 943–951.
[49] Y. Onose, Y. Ito, J. Kuwabara, T. Kanbara, Polym. Chem. 13 (2022) 5486–5493.
[50] J. Pyun, C. F. Carrozza, S. Silvano, L. Boggioni, S. Losio, A. R. d. Angelis and W. O. N. P. Jr, J. Polym. Sci. Part a-Polym. Chem. 60 (2022) 3471–3477.
[51] L.J. Dodd, Ö. Omar, X. Wu, T. Hasell, ACS Catal. 11 (2021) 4441–4455.
[52] C. Tavella, P. Lova, M. Marsotto, G. Luciano, M. Patrini, P. Stagnaro, D. Comoretto, Crystals 10 (2020) 1–10.
[53] V.S. Wadi, K.K. Jena, K. Halique, B. Rozic, L. Cmok, V. Tzitzios, S.M. Alhassan, Sci. Rep. 10 (2020) 1–12.
[54] R.M. Klevens, M.A. Morrison, J. Nadle, S. Petit, K. Gershman, S. Ray, L.H. Harrison, R. Lynfield, G. Dumyati, J.M. Townes, A.S. Craig, E.R. Zell, G.E. Fosheim, L. K. McDougal, R.B. Carey, S. Fridkin, JAMA 298 (2007) 1763–1771.